Exploratory study on how sub-ply fiber orientation affects the cracking behavior of wax-based barrier coatings

G. MARIN, A. HAGMAN, A.-K. ERIKSSON, E. PERSSON, C. RYDEFALK, AND P. SRINIVASA

ABSTRACT: The transition to 100% biobased packaging presents considerable challenges, particularly in the development of a petroleum-free barrier. Generally, biobased barriers exhibit lower flexibility compared to traditional barriers, thereby increasing the risk of cracking during the converting process.

The present study examines the possibility of optimizing the substrate to reduce cracking in brittle barriers. Five three-ply composites were fabricated using commercial paperboard to enable a composite with different fiber orientation in the individual plies. The different orientations achieved varying mechanical properties, including strain-at-break and folding resistance, with a ranking that is comparable to a standard multi-ply paperboard. The composites were subjected to creasing at five distinct depths to assess the area percent of barrier cracks across the crease bead. Micro-cracks appeared on the surface before larger coating cracks were registered. As expected, the area percent of barrier cracks increased significantly with greater creasing depths. The orientation of the bulky middle ply showed little difference in the cracking propensity. However, by replacing the stiffer bottom ply with a ply of lower stiffness, the cracking propensity was significantly reduced without a substantial loss in mechanical properties. Hence, these findings indicate that it is possible to reduce the cracks in the barrier by modifying the fiber orientation in the different plies.

Application: The present research provides an avenue for working with paperboard properties that enables biobased barriers.

Biobased barriers are materials that are derived from renewable plant-based sources, such as corn, wheat, and other crops. These barriers can be used in a variety of applications, including packaging, coatings, and insulation. They offer several benefits over traditional petroleum-based barriers, including being more environmentally friendly and sustainable. Biobased barriers can also be biodegradable and compostable, making them an eco-friendlier alternative to traditional materials.

Cracking or failure during the converting process of biobased barriers can occur due to a variety of factors. One of the main causes is the inherent brittleness of the bio-based materials used to make the barriers. These materials may not be as flexible as traditional petroleum-based materials and thus can be more susceptible to cracking under converting loads. The brittleness of biobased barriers compared to traditional petroleum-based barriers has been shown in previous studies [1-3]. Increasing the brittleness of the barrier has been shown to increase the crack area [4]. To minimize these issues, it's important to optimize the barrier and substrate (paperboard) combinations such that optimal choices of barrier and substrate combinations can be made.

Surface cracks on a folded edge can be macroscopic and both render the barrier non-functioning but also deter from the visual appearance of a printed surface. Cracks in the millimeter size have been studied by staining or printing the substrate before creasing and folding [5–7]. However, the cracks can also be microscopic, but still detrimental to the barrier integrity [3,4]. It is somewhat straightforward to evaluate the leakage through the barrier. However, to study the crack morphology or area percent of cracked barrier, optical microscopy and/or scanning electron microscopy are usually needed [4]. Studies have been made trying to use different computer-aided image evaluation techniques for quantitative characterization of fold cracks [8]. In the present study, a way to stain and visualize the micro-cracks was utilized, thereby enabling the study of several and larger surfaces.

Certain aspects of the paperboard substrate are known to be beneficial to the overall converting performance (i.e., reduced cracking tendency) of paperboard-barrier laminates. The fiber orientation in-plane is one of them. The manufacturing of paperboard aligns the fibers to a higher degree in the machine direction (MD) than the cross-machine direction (CD). Paperboards with several fiber-plies will still have the same general in-plane orientation in all of them. The fiber alignment is known to cause material anisotropy that affects the mechanical properties of the paperboard. The bending stiffness of the paperboard in MD is greater than CD due to the fiber alignment that resists folding [9]. Creasing parallel to the MD usually folds easier and causes less top layer damage [7]. In packaging production, however, the material will be creased and fold-

Board	Thickness (std), µm	Grammage, g/m²	Density, kg/m³
A: Top ply	316 (2)	252	798
B: Middle ply	410 (8)	272	663
C: Bottom ply	316 (2)	252	798

I. Properties of the paperboards in the study (std: standard deviation).

ed along both MD and CD, as well as along angles in between, to create a finished package. It is therefore of interest to investigate what happens to the cracking propensity when the fiber orientation in the different plies is altered.

The objective of this study was to study the cracking behavior of a biobased barrier due to the fiber orientation in the different paperboard plies. Is it possible to reduce the cracks by altering the fiber direction in different plies. Paperboard composites with different ply orientations were developed, utilizing identical raw materials in the plies.

MATERIALS

To study the effect of fiber orientation on barrier cracking propensity, composite sheets were constructed from commercial paperboards imitating the construction of a multiply paperboard.

List of paperboards

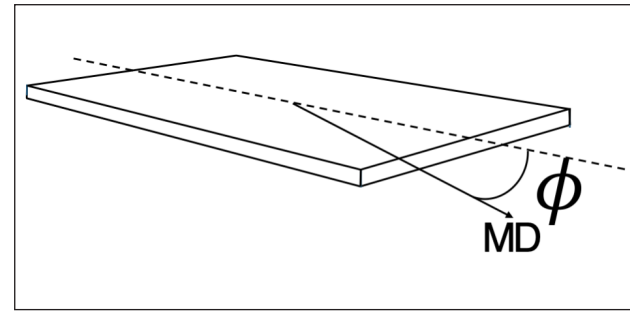
To create the composite sheets in this study, two distinct types of boards were utilized as primary materials. The first material is a commercially-produced coated folding boxboard (FBB) with a grammage of 235 g/m², which served as the outer plies of the composites. The second material is a commercially-produced cartonboard designed for hobbyist applications, utilized as a bulky middle ply. **Table I** shows the different boards. The configuration aimed to replicate the typical structure of commercial paperboard, characterized by a sandwich construction where the outer plies exhibit greater stiffness and strength compared to the bulkier middle ply. A coated FBB was selected to facilitate the barrier application. Both the FBB and the cartonboard were delivered in sheets, A0 and A4, respectively. It was assumed that the sheets were cut so that MD and CD were parallel to the edges of the sheets. A tensile test confirmed which direction was which.

Composites

Five different composites were constructed from the paperboards in Table I and are listed in **Table II**. The orientation was defined by the parameter ϕ, illustrated in **Fig. 1**. Hence, ϕ corresponds to a ply oriented in the MD and a value of 90° corresponds to the CD.

The composite sheets were glued together using wallpaper adhesive. The glue (51.5 g/m²) was applied to the sheet with an applicator to achieve an even layer. After placing the sheets together, a wide metal scrape was used to press out any bubbles and/or excess glue. The composites were then placed on a heat plate at 110°C between absorbent mats to remove the moisture from the glue. Weight was applied during drying to reduce curl. After drying, the composite samples were conditioned at 23°C and 50% relative humidity (RH) for at least 48 h before further testing.

Two possible risks were identified with regards to the glue influencing the results. The first one was that the glue would penetrate the fibers and form a continuous film/matrix with the fibers, and the test data would be a result of this structure, not the fibers. The second one was that the glue might increase the moisture too much in the fibers and thereby deteriorate the mechanical properties of the boards. However, the glue was starch based and not polymeric. Therefore, the glue should not form a continuous system



1. Definition of the sheet orientation (MD: machine direction) and the angle, Φ.

Composite (5 sheets of each)	Orientation Top Ply	Orientation Middle Ply	Orientation Bottom Ply	Thickness (std), µm	Coat Weight (std), g/m²
0-0-0	0	0	0	1124 (19)	5.2 (0.7)
45-45-45	45	45	45	1129 (25)	3.8 (0.5)
90-90-90	90	90	90	1113 (14)	5.4 (0.4)
0-0-90	0	0	90	1123 (26)	6.6 (0.7)
45-90-45	45	90	45	1090 (20)	5.1 (0.6)

II. Properties of the composites (std: standard deviation).

with the fibers. The starch in the glue might, however, strengthen the mechanical properties of the boards somewhat. Tensile tests were performed on paperboard sheets with and without glue (but without attaching another sheet), and the differences were insignificant. Soaking the fibers might change the properties; however, it was deemed consistent regardless of fiber direction. Since it is consistent, the moisture should not change the difference in properties between the different directions and layers. The moisture gradient introduced by the glue could have led to curl. To mitigate the possibility of curl, the sheets were dried with a weight after glueing. Since the composites were manually manufactured, the variation in thickness between them was greater than what is typically observed in commercially produced board. However, as shown in Table II, the difference in mean thickness between the thickest and thinnest composite is approximately 3.5%, which falls within the range of the standard deviation measured for the individual composites.

Thickness, grammage and density

The thickness measurements were performed using a thickness gauge from Lorentzen & Wettre (ABB; Stockholm), with a probe area of 2.27 cm^2 and nominal pressure of 50 kPa.

The thickness measurement was performed on five 25 cm × 15 cm (0.0375 m^2) sheets per quality, five points per sheet for the individual plies. The thicknesses of the individual plies are listed in Table I.

The grammage of the individual plies was calculated by weighing the five sheets from the thickness measurements on a Mettler AM50 laboratory scale (Mettler Toledo; Greifensee, Switzerland). The grammage and density of the materials were calculated and are reported in Table I.

METHODS

Mechanical characterization of the substrates

The materials used in this study were mechanically evaluated both as individual plies and as composites. For the separate plies, the material characterization was performed in MD, CD, and 45°, respectively. All tests were performed in standard climate, i.e., 23°C and 50% RH. It should be noted that except for the folding test, all evaluations were performed on creased, but unfolded, samples.

Tensile tests

Tensile tests were performed on both the individual plies and the composites. Measurements were carried out using a tensile tester manufactured by Lorentzen & Wettre that employs a span of 100 mm and a clamping pressure set at 6 bar. The testing procedure was displacement controlled at a rate of 100 mm/min. The resulting tensile curves were documented and analyzed using MATLAB Version R2023b (MathWorks; Natick, MA, USA), enabling the calculation of tensile stiffness, breaking strength, and strain at break.

The tensile properties of the individual plies were characterized in accordance with ISO 1924-3:2005 "Paper and board — Determination of tensile properties," using ten 15-mm-wide strips in MD, CD, and 45°, respectively. The tensile properties of the composites were evaluated on five 15-mm-wide strips from three separate composite sheets. The orientation in the length direction of the test strips was the same as the orientation listed in Table II.

Folding tests

The composites were folded using the two-point bending method described in ISO 5628 "Paper and board — Determination of bending stiffness — General principles for two-point, three-point and four-point methods." Five 15 mm × 100 mm test pieces from each composite were cut from two different sheets per orientation combination. Measurements were carried out using a bending tester from Marbach (Marbach Group; Heilbronn, Germany). The tests were performed with a bending length of 45 mm and a folding angle of 90°.

Barrier and barrier application

A commercial barrier solution was used in the present project. The barrier formulation is based on natural waxes to achieve the hydrophilicity of naturally occurring wax-impregnated materials.

The barrier solution was applied to the composites using a laboratory flexographic printing press, an IGT F1-100 (IGT Testing Systems; Almere, The Netherlands). The impression force on the print cylinder was 500 N, and the speed was 0.2 m/s. The print cylinder performed two pre-inking revolutions. The anilox volume was 8.5 mL/m^2, and it was run at 50% of the print cylinder speed with an anilox force of 250 N and five pre-inking revolutions. The barrier printing was performed in standard climate (50% RH at 23°C) after conditioning the samples for 24 h. Five samples per composite were printed. Having different orientations on the top layer during printing will affect the patterns in the barrier.

An important aspect of barrier application is applying a sufficient layer for the barrier to be effective. The target wet weight was therefore to apply at least 4 g/m^2 of the barrier solution. To enable the application of a thicker layer of solution, a flexible plastic blade was used as doctor blade. Additionally, the barrier solution was applied in several layers. Three coating layers were applied wet-in-wet. After each application the sample was weighed to assess the barrier coat weight. The resulting coat weight is presented in Table II. The average coat weight of the barrier varied a little between the different composites. However, there was no correlation seen between average coat weight and amount of cracking; i.e., there are composites with large differences in average coat weight, but small differences in the number of cracks.

Crack evaluation

Creasing

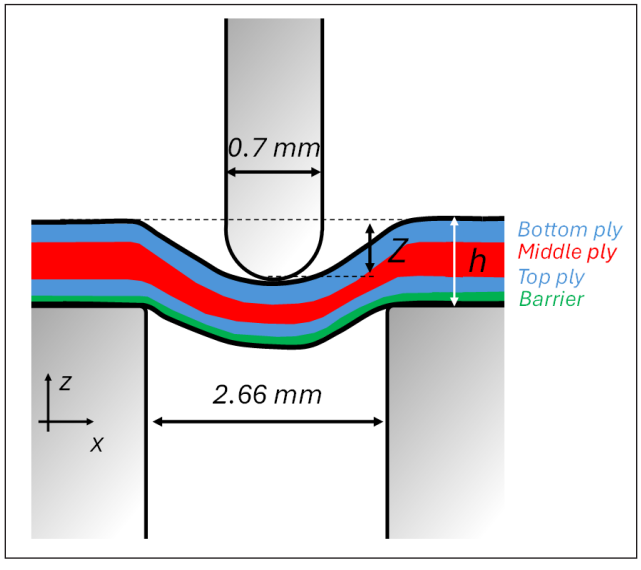
Creasing was performed on 25-mm-wide strips of the composite material. The barrier coated side of the composite was placed facing the channel. One strip was cut from each composite sheet, i.e., five strips per orientation combination were tested. Each strip was creased in five positions with increasing severity. The width of the ruler and channel in the creasing setup were kept constant, and the crease depth, *Z*, was adjusted, as illustrated in **Fig. 2**. The paperboard was fully constrained 50 mm to the right of the ruler and constrained in the *x*-direction on the left side, according to the coordinate system defined in Fig. 2. To account for the difference in thickness between the composite sheets, the ratio between crease depth *Z* and sheet thickness *h* was used (i.e., *Z/h*) to provide a comparable increase in creasing severity. The thickness of each test sample was measured before creasing, and the crease depth, *Z*, was adjusted accordingly.

To provide a spread of crack severity of the samples, five different *Z/h* ratios were chosen: 0.45, 0.91, 1.36, 1.82, and 2.27. The ratios were chosen based on an initial ocular investigation based on the damage of the largest creasing depth when creasing uncoated material, as to ensure that no surface cracks occurred in the substrate.

The creasing of the samples was performed in a universal testing machine, a Zwick Roell machine type Z005 (Zwick Roell Group; Ulm, Germany), together with an in-house built creasing setup. The ruler is attached to the piston and moves at a speed of 60 mm/min.

Measuring cracks

To locate the cracks in the barrier, the samples were dyed with a mix of 200 mL of water, 0.007% surfynol, and 0.15 g methylene blue. The dye works on the same principle as the mix utilized in the absorption variation method developed by Thorman [10]. The dye easily wets and stains the coating of the paperboard. Optimally, the dye would not stain the barrier at all, but unfortunately that is not the case here. However, the dye requires a longer contact time to stain the barrier, which therefore still makes it suitable for locating the cracks. The dye was applied with a saturated sponge covering the entire crease, ensuring liquid contact with the entire surface during the dyeing process. Since the dye stains both the barrier and the coating, the application needed to be timed. The timing was performed with a metronome, and the saturated sponge was in contact with the paperboard for eight beats at 120 bpm. Excess liquid was immediately removed using edge wicking of tissue paper, i.e., no additional pressure was applied.



2. Illustration of the creasing of samples, where* h *is the thickness of the sample and* Z *is the crease depth measured from the sample surface.

The stained samples were scanned in RGB 4800 dpi resolution using the Perfection v850 Pro scanner from Epson (Nagano, Japan) and the scanning software SilverFast v8.8 (LaserSoft Imaging; Kiel, Germany). Evaluation was performed in the program DotStat. DotStat is a program developed in-house by Innventia (now RISE Research Institutes of Sweden) as a research tool to study raster dots in halftone prints. A reference frame for the reflectance was scanned together with the samples, and a calibrated reflectance image in the red channel was used to threshold the image into binary data.

The barrier application process will affect the coverage and patterns in the barrier. The present project utilizes a flexographic print press to apply the barrier on the composite sheets. When the substrate leaves the print nip, the barrier solution is split between the paperboard and the print plate. In this splitting process, instabilities are formed that are known as Saffman-Taylor instabilities [11] or viscous fingers. The prominence and wavelengths of these patterns on a printed surface depends on, e.g., the viscosity of the transferred fluid [12]. The viscous fingers are visible to the naked eye at the right gloss angle, as seen in **Fig. 3**. This phenomenon highlights the difficulty of comparing the extent of cracking in the barrier when the top plies have different orientations. Therefore, it is essential to compare composites with the same top ply-orientation when evaluating crack formation.

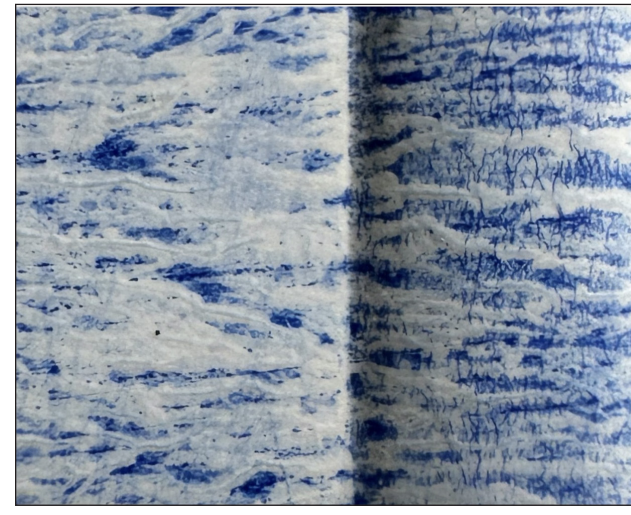
The finger pattern in the barrier coating will affect the dyeing process used to locate the cracks. As previously noted, the dye application required some contact time. The dye does not wet the barrier easily but does stain the surface. The dye will therefore easily migrate from the ridges in the viscous finger pattern down to the valleys. To mitigate the effect of the migration, the sponge was utilized rather than applying the dye with a pipette to ensure complete contact. The dyed cracks running perpendicular to the white finger pattern in the barrier are clearly visible to the right in **Fig. 4** and not present in the uncreased area to the left. However, the white horizontal streaks of the viscous fingers remain, and it is not



3. Viscous finger patterns in the barrier coating.

trivial to decide whether the lack of cracks across them (although there are some present) are due to ink migration/insufficient contact time, or whether the thicker part of the barrier has not cracked all the way down to the pigment coating or has not cracked at all. Examples of clear cracks running perpendicular across the finger pattern also exist, as seen in Fig. 4. It is, however, clear that the dye enables capture of the fine micro-cracks in the barrier where the pigment coating underneath might still be largely unaffected.

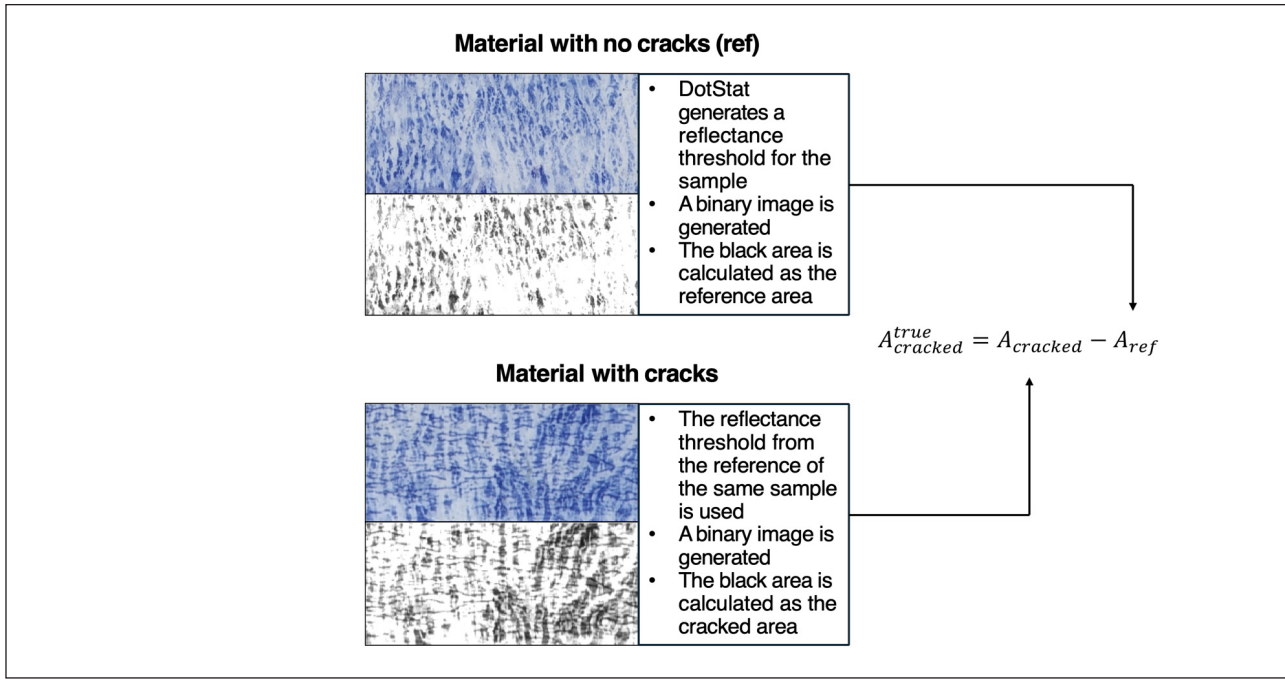
The reflectance of the dyed cracks is locally lower than the surrounding area, thereby making the cracks obvious to the naked eye. Evaluating the cracks programmatically requires a reflectance threshold to separate cracked and uncracked surface. However, the cracked area might not have the lowest reflection seen to the whole scanned area, which adds an additional difficulty in evaluating the amount of cracking in the barrier; i.e., a clearly visible crack has a lower reflectance than its immediate surroundings. However, in another location on the same crease, another visible crack runs through, e.g., a valley and both the crack and its surroundings have a lower reflectance than the other crack. Setting a global reflectance threshold is therefore difficult, as it will either remove large portions of the cracked area or include uncracked darker areas. The amount of dark background and the level of background variation differ between the different sheets. To account for this, an uncreased but dyed area on each strip was evaluated. At the selected reflectance threshold, the area percent dyed area is calculated from the uncracked sample. It is then assumed that this amount of dyed area will be the same for all creases on the same strip and the area percent of the uncracked, dyed area is subtracted from the thresholded reflectance of the cracked sample. The procedure is visualized in **Fig. 5**.



4. Left: dyed, un-creased (un-cracked) area. Right: crease with visible cracks.

Comparison of digital and ocular crack detection

To validate the quantitative approach used in this study, a reference group of six participants was asked to observe a subset of the same images that were analyzed by the software. The participants were asked to do pairwise comparisons of cracked areas and decide which was more cracked. The participants were shown an enlarged section of the middle of the crease from all samples, which is in contrast to the image analysis that analyzed the whole width. The result was then compared to how the image analysis had ranked the two pictures. The picture pairs were chosen so that both pictures were from the same crease depth and compared Composite 0-0-0 and Composite 0-0-90. The composites were chosen since they had the same top-ply orientation. This selection was made to make a preliminary verification of the image analysis.



5. Flowchart for calculating the cracked area.

RESULTS AND DISCUSSION

Tensile properties

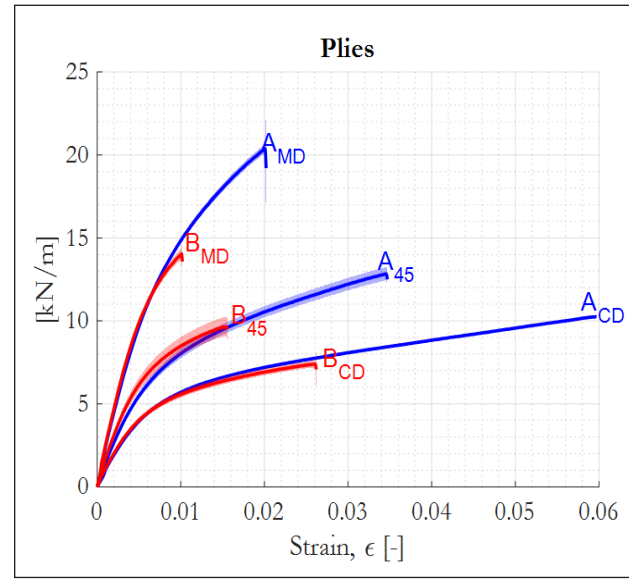
A typical commercial paperboard has a higher tensile strength and stiffness in MD than CD, but a higher strain at break in CD than in MD due to the fiber alignment in the plane. A tensile test conducted in the 45° direction is expected to fall in between the MD and CD properties.

Both paperboards in the present study show the expected tensile behavior in MD-CD, as shown in **Fig. 6**. The standard deviation is shown as a shaded area but is only large enough to be visible in the 45° direction. This confirms the desired fiber orientation of the composites.

The paperboards in the study were selected to produce a composite with a weaker, bulkier middle ply and thinner, stronger outer plies. The tensile tests in Fig. 6 findings show that the outer plies (Paperboard A) exhibit markedly greater strength and strain-at-break compared to the middle ply (Paperboard B), a trend consistent across all tested directions. This confirms the desired construction of the composites.

The tensile curves for the various composites are presented in **Fig. 7**. It is observed that the composites in which all plies are oriented in the machine direction (0-0-0) exhibit the highest strength alongside the lowest strain-at-break. Conversely, Composite 90-90-90 demonstrates the lowest strength but attains the greatest strain-at-break. This trend is corroborated by the stress-strain curves illustrated in Fig. 6.

Composite 45-45-45 exhibits the same behavior as the paperboard tested in the 45° direction. The composite falls in the middle with a larger strain at break than 0-0-0, but

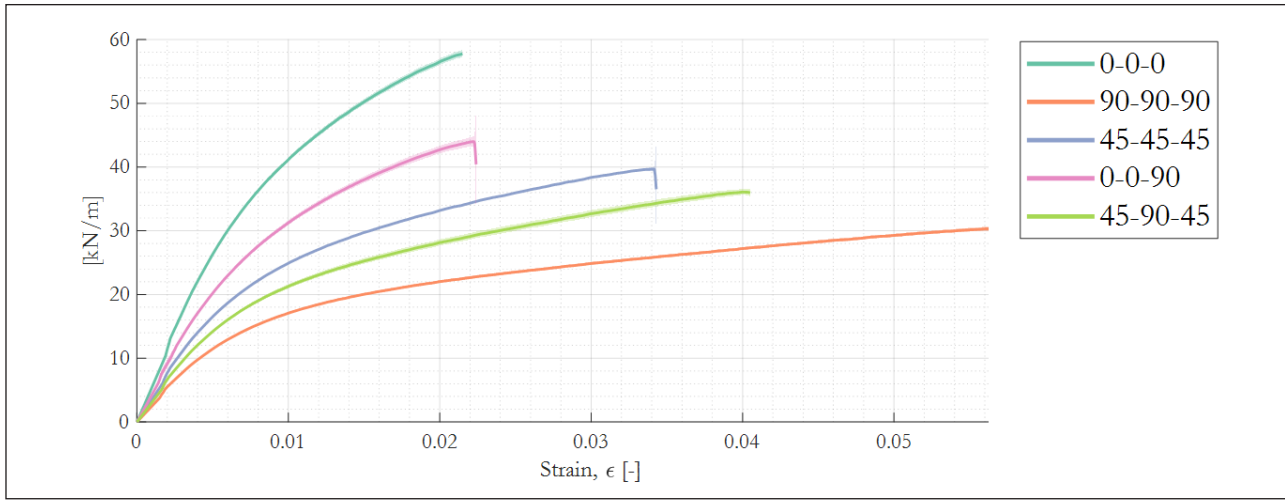


6. Load-strain curves of the different paperboards in machine direction (MD), cross-machine direction (CD), and 45°, respectively.

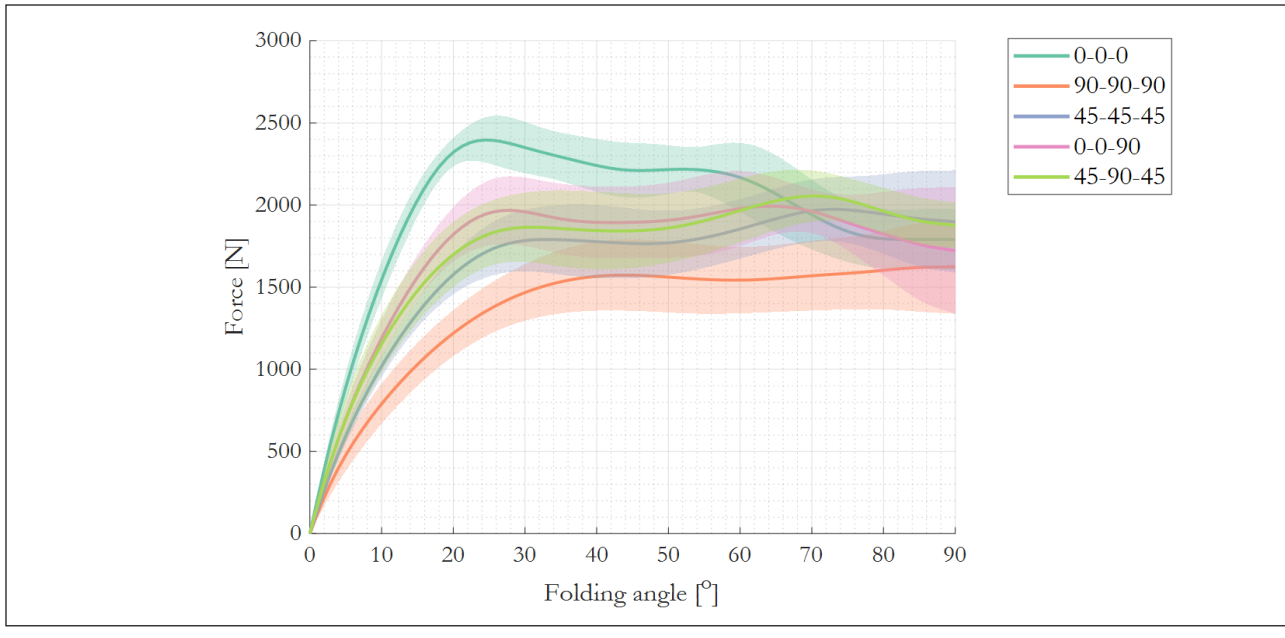
not as long as 90-90-90. The strength and stiffness are larger than 90-90-90, but not as large as 0-0-0. The results clearly illustrate the typical behavior of having most of the fibers aligned in the same direction.

For Composite 0-0-90, it was observed that compared to Composite 0-0-0, strain at break remained unaffected; however, there was a reduction in strength. This behavior is logical, as the top ply oriented in the machine direction is anticipated to fail at approximately 2% strain, resulting in the subsequent failure of the underlying ply.

Composite 45-90-45 exhibited a stress-strain curve sim-



7. Stress-strain curves of the different composites.



8. Folding curves for the different composites.

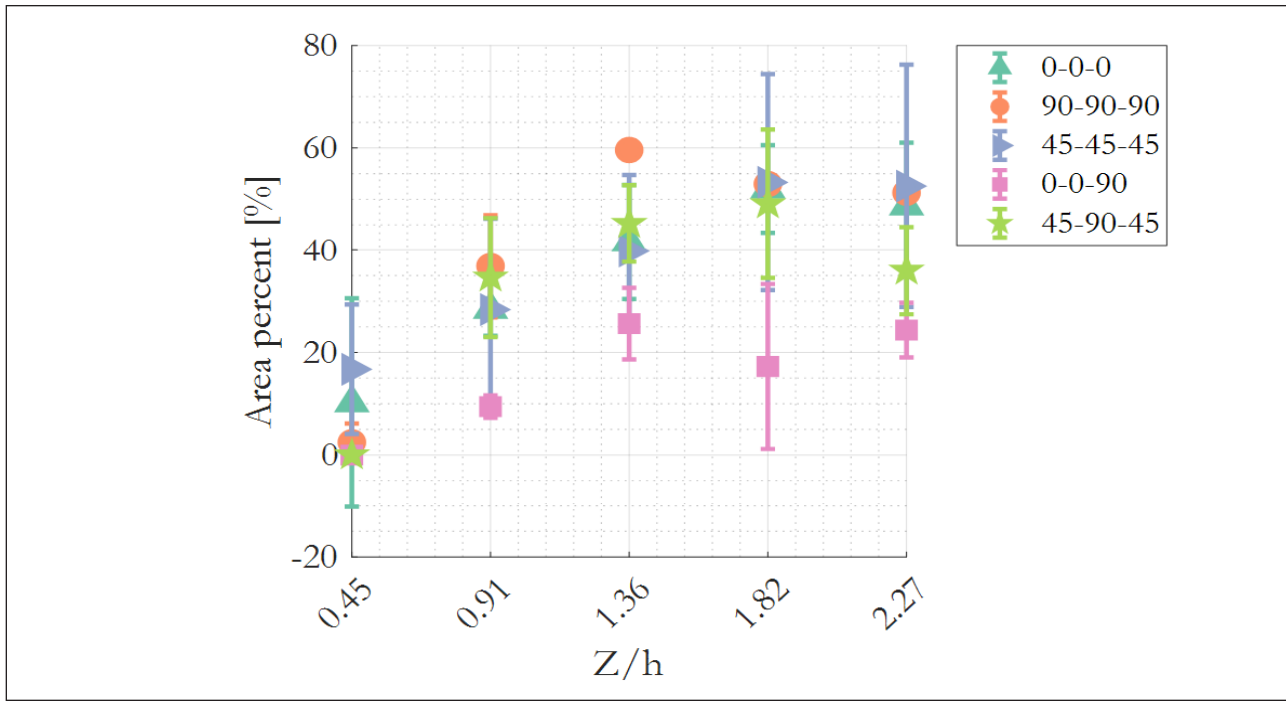
ilar to that of Composite 45-45-45, yet with a greater strain and slightly reduced strength, a phenomenon expected due to the orientation of the middle ply.

Overall, there is a distinct differentiation in the in-plane properties among the five composites analyzed. The ranking remains the same between the composites exhibiting the same fiber directions as in the paper board tensile test. The two composites with mixed directions are therefore expected to provide information on the creasability of crossed fiber layers.

Folding resistance

In the folding tests, the differentiation among the various composites was less pronounced compared to the tensile tests. Composite 0-0-0 exhibited the highest resistance to bending, while Composite 90-90-90 displayed the lowest, as is shown in **Fig. 8**. The results concur with both theory and the tensile test results. Folding the 0-0-0 composite means folding across the fiber direction, and it is seen to be the stiffest. Folding the 90-90-90 composite means folding alongside the fiber direction, and this composite is the weakest.

The remaining three composites included in the study demonstrated values between 0-0-0 and 90-90-90 in the same way they did in the tensile tests. However, the distinction between Composites 45-45-45, 0-0-90, and 45-90-45 is not as clear as in the tensile tests. The standard deviation of the three composites is largely overlapping. Additionally, the standard deviations for the folding tests were significantly greater than those for the tensile tests. Typically, standard deviations in such tests tend to be larger, and in this study, the variability may have been exacerbated due



9. Area percent cracks for all the different composites.

to differences in thickness arising from the manual fabrication of the composites. It is important to note that thickness plays a critical role in determining folding resistance. However, the overall ranking with unidirectional fibers at each end and the directionally twisted composites in between remains.

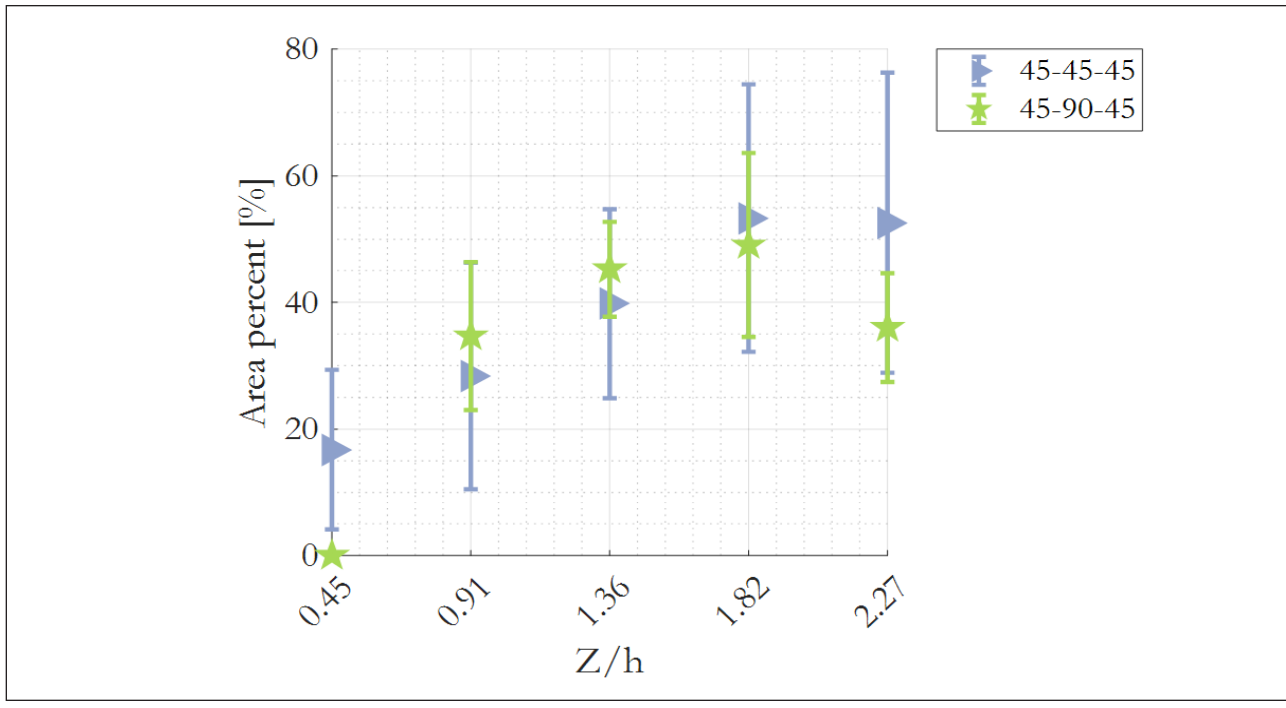
Creasing and crack evaluation

To assess the effect of rotated fiber direction, the cracked area was evaluated for increasing crease depths. Typically, at the lowest creasing depth, defined by a *Z/h* ratio of 0.45, the appearance corresponds to the reference image in Fig. 5, i.e., the viscous finger pattern within the barrier coating is distinctly observable, while no cracks are present. When increasing the creasing depth, the number of cracks generally increased as well.

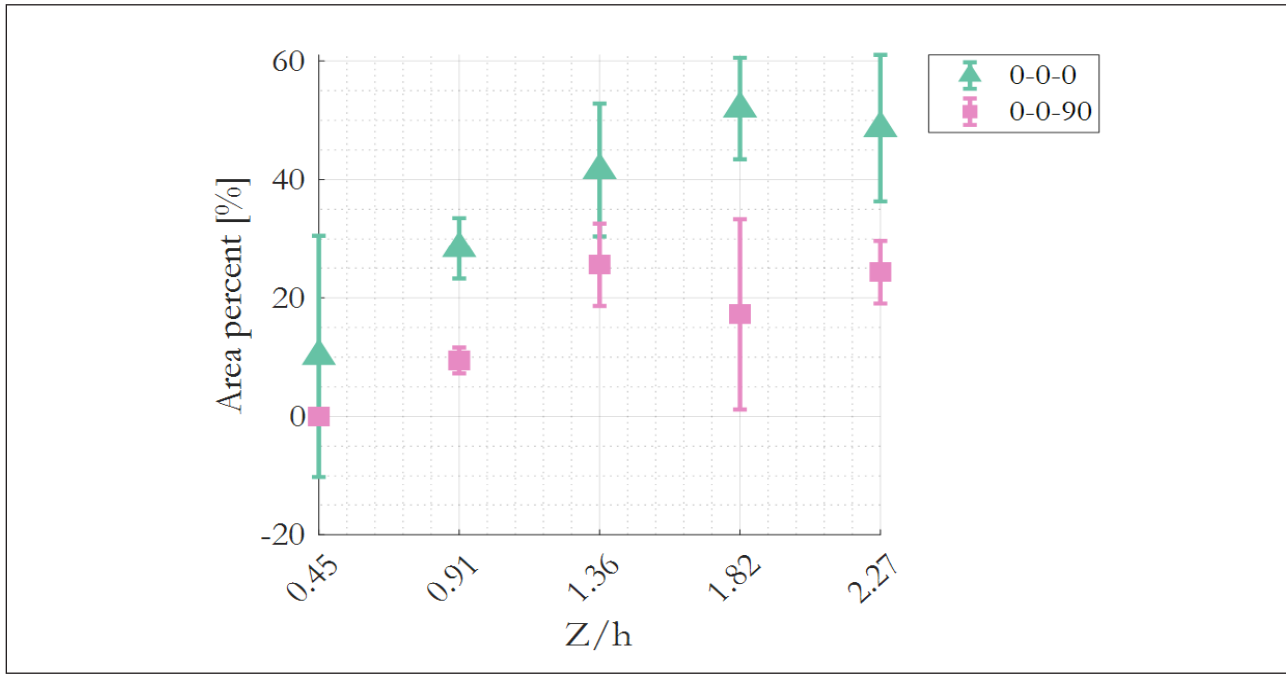
The area of cracking was assessed in relation to various *Z/h* ratios, with the results presented in **Fig. 9**. As seen in Fig. 9, a discernible trend emerges whereby the cracked area exhibits an initial increase corresponding to higher *Z/h* ratios. Furthermore, it was observed that the area of cracking increased rapidly with the *Z/h* ratios between 0.45 to 0.91. This pattern is consistent across all composite materials examined, up to the second largest depth; notably, there is no significant variation between the *Z/h* ratios of 1.82 and 2.27. This observation may be attributed to the fact that the barrier is fully compromised at these levels. The observed increase in cracked area with deeper creasing suggests that the proposed measurement method for quantifying cracks is effective. Nonetheless, it is important to note that Fig. 9 does not reveal any notable differences among the composites. This lack of differentiation may stem from the challenges associated with optically analyzing barrier cracks across varying fiber orientations in the top ply, as these orientations can influence the application of the barrier.

Hence, it is of interest to evaluate the composites with the same orientation in the top ply; i.e., the ply on which the barrier is applied. The cracked area for the two composites with a 45° direction top ply are shown in **Fig. 10**. The composites demonstrate comparable responses during the creasing procedure, making differentiation challenging, particularly in light of the substantial standard deviations observed. This phenomenon may be attributed to the fact that the only difference between the two composites is the orientation of the weaker middle ply. The tensile behavior in Fig. 7 shows how the weaker middle ply reduces the stiffness and strength of 45-90-45 compared to 45-45-45. However, the folding resistance, as shown in Fig. 8, is not significantly different between the two composites. Consequently, it is anticipated that the resulting curves will exhibit similarities, as the role of the middle ply primarily serves to augment bulk rather than to influence mechanical properties to any large extent.

For the two composites featuring a top ply oriented at 0°, one of them has a bottom ply oriented at 90°. Changing the fiber direction of the bottom ply significantly impacts the resulting cracked area percent, as shown in **Fig. 11**. By altering the bottom ply, the tensile properties are reduced somewhat, as can be seen in Fig. 7. However, by changing the direction of the bottom ply, the folding resistance is also reduced, as seen in Fig. 8. Hence, these find-



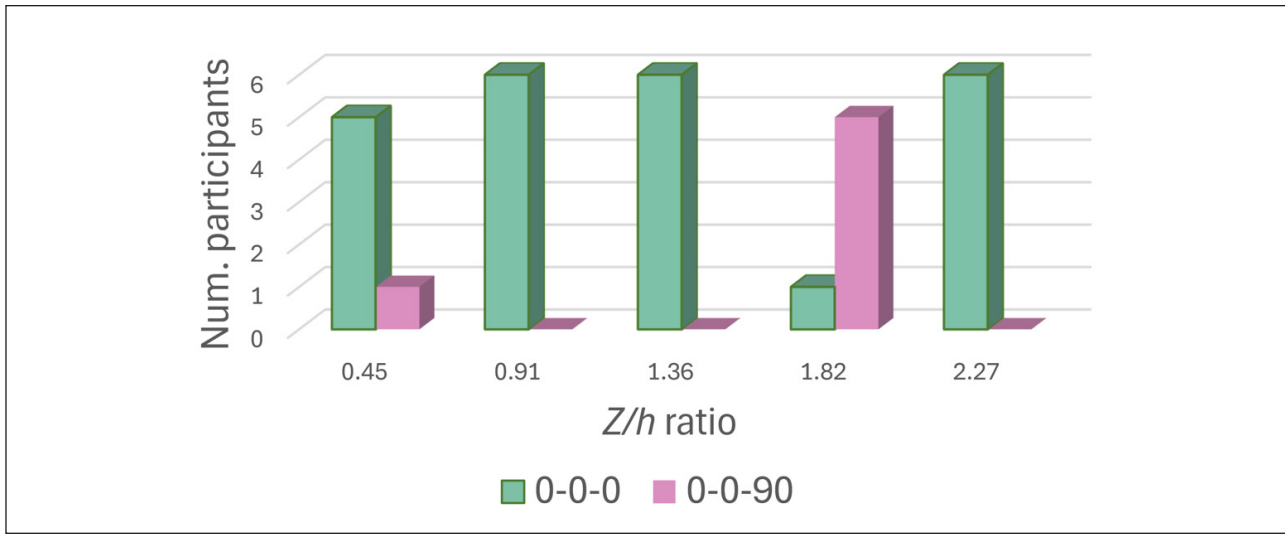
10. Area percent cracks for samples with 45° top side direction.



11. Area percent cracks for samples with 0° top side direction.

ings indicate that it is possible to reduce the cracks in the barrier by modifying the fiber orientation in the bottom ply provided that the tensile properties of the board can be reduced an acceptable amount.

The reference panel compared pictures of the cracked barriers from Composite 0-0-0 and Composite 0-0-90 at the same creasing depths. The results from the panel are shown in **Fig. 12**. The panel participants are in full agreement for three out of five pairs. In two cases, *Z/h* ratio 0.45 and 1.82, only one participant deviated from the consensus. When Fig. 12 is compared to Fig. 11, it is clear that the panel's assessments align well with the quantitative method. However, there is one notable exception at the second-highest creasing depth (1.82), where the majority of the panel judged Composite 0-0-90 to be more affected. For all creasing depths except this one, the panel's evaluations are con-



12. Subjective ranking of cracks, comparing Composite 0-0-0 and Composite 0-0-90.

sistent with the software's analysis. In the case of the outlier, the standard deviation in the software's results is relatively high, and a substantial number of cracks were observed at this creasing depth. This suggests that the images presented to the panel may have been more difficult to distinguish at this level of damage.

These findings hint at two possible mechanisms that influence the strain state in the barrier. The change in fiber direction in the underlaying plies changes the stiffness of those layers in the 0-direction. This leads to a reduced overall stiffness of the total composite, which allows for more material to be fed into the crease tool during creasing, thus reducing the overall strain on the composite. However, as the barrier carrying layer is the same, the localized straining behavior remains unchanged; i.e., the tensile stresses close to the barrier decrease without reducing the stiffness the same amount, thus reducing the local tensile strain in the barrier. Another possible mechanism is that the change in stiffness profile through the board will lead to increased shear stresses, which in turn will provoke delamination that helps alleviate the tensile stresses on the barrier carrying layer.

CONCLUSIONS

The objective of this study was to examine the change in cracking propensity of a wax-based barrier when the fiber orientation of the sub-plies of the paperboard substrate is altered. A total of five paperboard composites were manufactured and creased to five crease depths.

A quantitative method to measure the amount of cracking was developed and shown to correlate to subjective comparison of crease severity.

It was shown that it was possible to reduce the cracking propensity by altering the fiber orientation of the bottom layer, i.e., the layer furthest away from the barrier, making it less stiff.

It was further shown that similar adjustments to the middle layer had a smaller effect on the cracking propensity; however, it should be noted that this layer is less stiff to begin with, and the fiber direction was altered to a lesser degree.

Clarifying the mechanisms that influence barrier damage deserve to be explored further, possibly by looking at more combinations of sublayer configurations for a known barrier carrying layer, preferably while examining the shear strength profile of the composite. This would also be a chance to examine the effect using industrially realistic changes in fiber orientation.

ACKNOWLEDGEMENTS

This project received funding from Stiftelsen Nils och Dorthi Troëdssons Forskningsfond, and the authors wish to express their sincere appreciation for this generous support.

CONTRIBUTIONS

The following people have contributed to the present work according to CRediT (Contributor Roles Taxonomy).

- Dr. Prashanth Srinivasa: Conceptualization, formal analysis, and funding acquisition.
- Dr. Gustav Marin: Data curation, formal analysis, methodology, project administration, software, supervision, validation, visualization, writing – original draft, writing – review & editing.
- Dr. Anton Hagman: Conceptualization, data curation, formal analysis, funding acquisition, methodology, project administration, software, supervision, validation, writing – original draft, writing – review & editing.
- Elsa Persson: Investigation, validation.
- Anna-Karin Eriksson: Investigation.
- Dr. Cecilia Rydefalk: Formal analysis, investigation, methodology, software, validation, visualization, writing – original draft, writing – review & editing.

LITERATURE CITED

1. Lev, R., Lyytikäinen, J., Matthews, S., et al., *Packag. Technol. Sci.* 37(11): 1037(2024). https://doi.org/10.1002/pts.2845.
2. Lev, R., Tanninen, P., Lyytikäinen, J., et al., *BioResources* 18(4): 8707(2023). https://doi.org/10.15376/biores.18.4.Lev.
3. Tanninen, P., Saukkonen, E., Leminen, V., et al., *Nord. Pulp Pap. Res. J.* 30(2): 336(2015). https://doi.org/10.3183/npprj-2015-30-02-p336-343.
4. Javed, A., Rättö, P., Järnström, L., et al., *Nord. Pulp Pap. Res. J.* 33(2): 336(2018). https://doi.org/10.1515/npprj-2018-3039.
5. Panek, J., Smith, S.D., and Coffin, D.W., *TAPPI J.* 19(4): 219(2020). https://doi.org/10.32964/TJ19.4.219.
6. Rättö, P., Hornatowska, J., and Barbier, C., *Nord. Pulp Pap. Res. J.* 27(4): 714(2012). https://doi.org/10.3183/npprj-2012-27-04-p714-720.
7. Bota, J., Pibernik, J., Kovačević, D., et al., "The effects of flatbed creasing tool on printed paperboard," *Proc., 11th Int. Symp. GRID*, University of Novi Sad, Faculty of Technical Sciences, Department of Graphic Engineering and Design, Novi Sad, Serbia, 2022, p. 657. https://doi.org/10.24867/GRID-2022-p71.
8. Pál, M., Dedijer, S., László, K., et al., *Nord. Pulp Pap. Res. J.* 36(4): 626(2021). https://doi.org/10.1515/npprj-2021-0041.
9. Nygårds, M., Bhattacharya, A., and Krishnan, S.V.R., *Nord. Pulp Pap. Res. J.* 29(3): 510(2014). https://doi.org/10.3183/npprj-2014-29-03-p510-520.
10. Thorman, S., Ström, G., Hagberg, A., et al., *Nord. Pulp Pap. Res. J.* 27(2): 459(2012). https://doi.org/10.3183/npprj-2012-27-02-p459-465.
11. Saffman, P.G. and Taylor, G., *Proc. R. Soc. London, Ser. A* 245(1242): 312(1958). https://doi.org/10.1098/rspa.1958.0085.
12. Brumm, P., Sauer, H.M., and Dörsam, E., *Colloids Interfaces* 3(1): 37(2019). https://doi.org/10.3390/colloids3010037.

ABOUT THIS PAPER

Cite this article as:
Marin, G., Hagman, A., Eriksson, A.-K., et al., *TAPPI J.* 25(5): 267(2026). https://doi.org/10.32964/TJ25.5.267

DOI: https://doi.org/10.32964/TJ25.5.267

ISSN: 0734-1415

Publisher: TAPPI Press

Copyright: ©TAPPI Press 2026

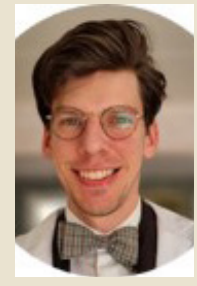
About this journal

ABOUT THE AUTHORS

We studied this topic because bio-based barriers are an important aspect of advancing the applications of paper-based products. Bio-based barriers are known to be brittle in comparison to more traditional barriers and therefore more prone to cracking during creasing. Additionally, previous research has shown that there are preferential directions when creasing paperboard with regards to cracking. What we have contributed is a look at what happens when the fiber directions are not consistent in the ply structure of the paperboard.

Development of the method presented here was the largest and most difficult part of the project. Through this study, we discovered that the fiber direction beneath the clay coating will affect the Saffman-Taylor instabilities in the barrier application. A particularly interesting finding was that it might be possible to reduce the cracking tendency by changing the fiber direction in the bottom ply. For mills, this indicates that there might be a way to reduce the cracking tendencies during paperboard converting (creasing). Our next step is to consider the effects of moisture.

Marin is a researcher; Hangman is senior researcher; Eriksson is research engineer; Persson is research engineer; Rydefalk is a researcher; and Srinivasa is senior researcher at RISE Research Institutes of Sweden in Stockholm. Email Rydefalk at cecilia.rydefalk@ri.se.



Marin



Hagman



Eriksson



Persson



Rydefalk



Srinivasa